

Topochemical Control of Covalent Bond Formation by Dihydrogen Bonding

Radu Custelcean and James E. Jackson*

Contribution from the Department of Chemistry, Michigan State University, East Lansing, Michigan 48824-1322

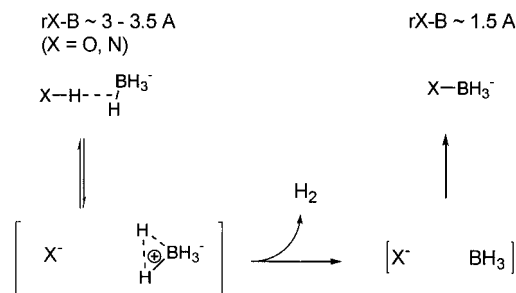
Received August 17, 1998

Abstract: This report explores the potential of the unconventional hydrogen bonds between the hydridic hydrogens in $X-BH_3^-$ ($X = H, CN$) and traditional OH or NH proton donors (dihydrogen bonds) to serve as preorganizing interactions for the topochemical assembly of covalent materials. Evidence for such topochemical control in the reaction $B-H\cdots H-X \rightarrow B-X + H_2$ was obtained in studies of the solid-state structures and reactivities of *N*-[2-(6-aminopyridyl)]acetamidine (NAPA) cyanoborohydride and triethanolamine (TEA) complexes of $NaBH_4$ and $NaCNBH_3$. The X-ray crystal structures of all three new compounds studied exhibit multiple dihydrogen bonds which are significant in defining the packing of the molecules in the solid state. Moreover, this new type of interaction is a powerful tool for crystal engineering; as planned, NAPA H_3BCN crystallized in the desired $(NAPA H_3BCN)_2$ closed loop coordination. Solid-state decomposition of $NaBH_4 \cdot TEA$ is topochemical, leading to a trialkoxyborohydride, which is not achievable in solution or melt. In addition to close H–H contacts, the relative acidity/basicity of the proton–hydride pairs make a significant contribution to the solid-state reactivity of dihydrogen-bonded systems, as demonstrated by the contrasting reactivities of the $NaBH_4 \cdot TEA$ and $NaCNBH_3 \cdot TEA$ complexes.

We have recently demonstrated, using X-ray and neutron diffraction,¹ IR and NMR spectroscopy, and ab initio calculations,² that the hydridic hydrogens, or more accurately the B–H electron pairs in the BH_4^- anion, can serve as the electron donors of a new type of hydrogen bond (dihydrogen bonding). In this new type of intermolecular interaction, the σ -bonding electron pair of a B–H bond (or other M–H where M is less electronegative than H) associates with a traditional H-bonding partner H–X ($X = N, O, \text{halogen}$). The same kind of interaction was independently noted by Crabtree et al.³ and Morris et al.⁴ in organoiridium and organorhenium complexes, and by Epstein et al. in organorhenium and organotungsten compounds.⁵ With H \cdots H distances of 1.7–2.2 Å and strengths of 4–7 kcal/mol, dihydrogen bonds are comparable with conventional hydrogen bonds.

Besides the control of chemical reactivity and stereoselectivity in solution,⁶ this new phenomenon has interesting implications for topochemically directed assembly of covalent materials. Such weak associations, in principle, may be used to organize and hold a structure's form while it is more firmly fastened together. A number of researchers have used H-bonding interactions to juxtapose sites that may then be photodimerized or polymerized

Scheme 1



into covalent structures.⁷ A general weakness of the systems studied to date, however, is the complexity or the low dimensionality of the preorganizing/coupling subunits.

Dihydrogen bonds represent an especially simple preorganizing interaction. In general, heating these systems drives off H_2 , leaving Lewis acidic and basic sites in close proximity. These subunits may combine to form strong covalent bonds, reflecting the connectivity of the original network. Scheme 1 shows how these systems are expected to lose H_2 , based on the known BH_4^- hydrolysis mechanism.⁸ The initial order dictated by H \cdots H interactions may thus be transferred to the newly formed covalent frame. This makes dihydrogen bonding a potentially powerful tool for rational assembly of new materials with crystalline, three-dimensional, covalent structures. Such substances typically have special heat transfer, hardness, or electronic characteristics—cf. diamond, silicon carbide, quartz,

(1) Jackson, J. E. et al. Manuscript in preparation.
 (2) Jackson, J. E. et al. Unpublished results. For similar studies see also: Epstein, L. M.; Shubina, E. S.; Bakhmutova, E. V.; Saitkulova, L. N.; Bakhmutov, V. I.; Chistyakov, A. L.; Stankevich, I. V. *Inorg. Chem.* **1998**, *37*, 3013.
 (3) Crabtree, R. H.; Siegbahn, P. E. M.; Eisenstein, O.; Rheingold, A. L.; Koetzle, T. F. *Acc. Chem. Res.* **1996**, *29*, 348.
 (4) Lough, A. J.; Park, S.; Ramachandran, R.; Morris, R. H. *J. Am. Chem. Soc.* **1994**, *116*, 8356.
 (5) (a) Shubina, E. S.; Belkova, N. V.; Krylov, A. N.; Vorontsov, E. V.; Epstein, L. M.; Gusev, D. G.; Niedermann, M.; Berke, H. *J. Am. Chem. Soc.* **1996**, *118*, 1105. (b) Belkova, N. V.; Shubina, E. S.; Ionidis, A. V.; Epstein, L. M.; Jacobsen, H.; Messmer, A.; Berke, H. *Inorg. Chem.* **1997**, *36*, 1522.
 (6) Gatling, S.; Jackson, J. E. Manuscript in preparation.

(7) (a) Feldman, K. S.; Campbell, R. F.; Saunders, J. C.; Ahn, C.; Masters, K. M. *J. Org. Chem.* **1997**, *62*, 8814. (b) Kane, J. J.; Liao, R. F.; Lauher, J. W.; Fowler, F. W. *J. Am. Chem. Soc.* **1995**, *117*, 12003.
 (8) (a) Pepperberg, I. M.; Halgren, T. A.; Lipscomb, W. N. *J. Am. Chem. Soc.* **1976**, *98*, 3442. (b) Schreiner, P. R.; Schaefer, H. F.; Schleyer, P. R. *J. Chem. Phys.* **1994**, *101*, 7625.

Table 1. Crystallographic Data for 1, 2, and 3

	1	2	3
formula	C ₈ H ₁₄ N ₅ B	C ₆ H ₁₉ NO ₃ BNa	C ₇ H ₁₈ N ₂ O ₃ BNa
formula wt	191.05	187.02	212.03
color, shape	clear, needle	clear, prism	clear, prism
dimens, mm	0.60 × 0.30 × 0.15	0.52 × 0.38 × 0.31	0.62 × 0.18 × 0.10
crystal system	triclinic	monoclinic	monoclinic
space group, Z	<i>P</i> $\bar{1}$, 4	<i>P</i> 2 ₁ / <i>n</i> (no.14), 4	<i>P</i> 2 ₁ / <i>c</i> (no.14), 4
<i>a</i> , Å	7.104(2)	9.23510(10)	7.55160(10)
<i>b</i> , Å	9.390(4)	7.35120(10)	15.1232(2)
<i>c</i> , Å	17.736(10)	15.8083(2)	10.57070(10)
α , deg	99.38(4)	90	90
β , deg	95.99(4)	103.6880(10)	105.5380(10)
γ , deg	111.53(3)	90	90
<i>V</i> , Å ³	1068.3(9)	1042.73(2)	1163.10(2)
temp, K	143(2)	173(2)	173(2)
<i>d</i> _{calcd} , g/cm ⁻³	1.188	1.191	1.211
no. of reflns collected	3118	9787	9974
no. of unique reflns	3095 (<i>R</i> _{int} = 0.0469)	2488 (<i>R</i> _{int} = 0.0211)	2753 (<i>R</i> _{int} = 0.0549)
2 θ _{max} , deg	56.94	56.30	56.34
no. of parameters	366	186	199
<i>R</i> ₁ , ^a <i>wR</i> ₂ ^b (<i>I</i> > 2 σ (<i>I</i>))	0.0454, 0.1110	0.0250, 0.0726	0.0352, 0.0891
<i>R</i> ₁ , <i>wR</i> ₂ (all data)	0.0577, 0.1212	0.0292, 0.0743	0.0442, 0.0945
goodness of fit	1.112	1.060	1.053

$$^a R_1 = \sum(|F_o| - |F_c|)/\sum|F_o|. \quad ^b wR_2 = \{\sum[w(F_o^2 - F_c^2)^2]/\sum[w(F_o^2)]\}^{1/2}.$$

boron nitride, gallium nitride. Their syntheses, however, usually require extreme temperatures and/or pressures, conditions that do not permit intentional incorporation of more delicate, complex structures. A low-temperature solid-state route to such compounds would thus enable the application of the well-developed tools of molecular synthesis to the construction of crystalline covalent solids.

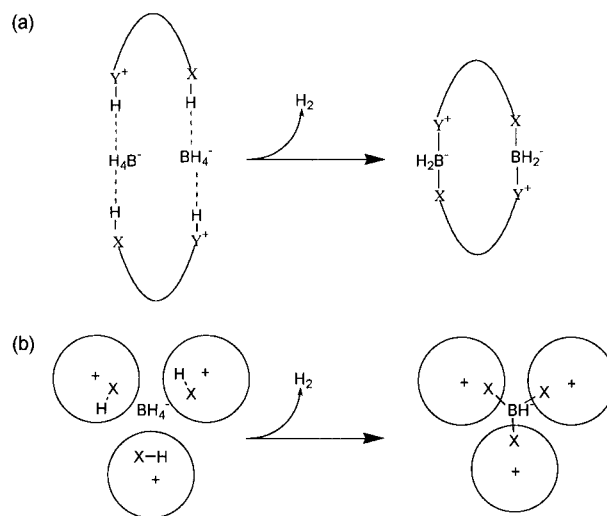
In the topochemical transformation outlined above, the initial H-bond arrangement should determine the final covalent structure. However, when going from the B–H···H–X interaction to a covalent B–X bond there is approximately a 2 Å change in distance between B and X, as illustrated in Scheme 1. This is a considerable shrinkage, and if it were cumulative in the reaction direction, it would lead to significant strain in the crystal as the new covalent network grew, with eventual loss of lattice control over the reaction. Even under these conditions, however, reactions may still be topochemical. A recent example is the thermal decomposition of cyclotrigallazane, [H₂GaNH₂]₃, leading to nanocrystalline gallium nitride.⁹ The neutron diffraction crystal structure of the starting compound showed short H–H contacts between Ga–H and H–N. Initial loss of H₂ at 150 °C resulted in an amorphous GaN phase. However, subsequent annealing at 600 °C for 4 h led to the unprecedented crystalline cubic gallium nitride (as about 50% of the GaN product). Despite the huge contraction of the unit cell, this reaction represents an overall topochemical loss of H₂ with Ga–N bond formation. The majority of organic compounds, however, cannot tolerate temperatures as high as 600 °C. Therefore, the challenge is to select systems with geometries and crystal packings that would topochemically lead to ordered covalent materials at relatively low temperatures in much the same way that carefully designed bifunctional monomers have given access to crystalline polymers.¹⁰ We are exploring two strategies to address this challenge:

(1) design of candidate cations to form closed loops in coordination with hydride-bearing anions (Scheme 2a)—in this case H₂ loss would lead to discrete molecular products which

(9) (a) Hwang, J. W.; Campbell, J. P.; Kozubowski, J.; Hanson, S. A.; Evans, J. F.; Gladfelter, W. L. *Chem. Mater.* **1995**, *7*, 517. (b) Campbell, J. P.; Hwang, J. W.; Young, V. G.; Von Dreelle, R. B.; Cramer, C. J.; Gladfelter, W. L. *J. Am. Chem. Soc.* **1998**, *120*, 521.

(10) Wegner, G. *Pure Appl. Chem.* **1977**, *49*, 443.

Scheme 2



are likely to be structurally different from the solution products, and lattice distortion would not be cumulative; and (2) selection of globular cations large enough that their close packing determines the lattice parameters, with the hydridic anions fitting into the interstitial holes (Scheme 2b)—bond formation via flexible arms would thus induce minimal change in the unit cell dimensions.

Results and Discussion

Crystal Engineering with Dihydrogen Bonds. Synthesis and Characterization of *N*-[2-(6-Aminopyridyl)]acetamidine (NAPA) Cyanoborohydride (1). NAPA H₃BCN was synthesized (Scheme 3) to test the ability of the cyanoborohydride anion to form dihydrogen bonds, as well as to explore the prospect of convergent coordination in closed loops. The white crystalline compound melts at 119–120 °C with decomposition and gas evolution. The ¹H, ¹³C, and ¹¹B NMR as well as IR spectra confirmed its structure. Figure 1 shows the X-ray structure for this compound. There are two independent centrosymmetric (NAPA H₃BCN)₂ dimers in the unit cell, each of them exhibiting close H–H contacts: 1.98, 2.12, 2.26 Å, and

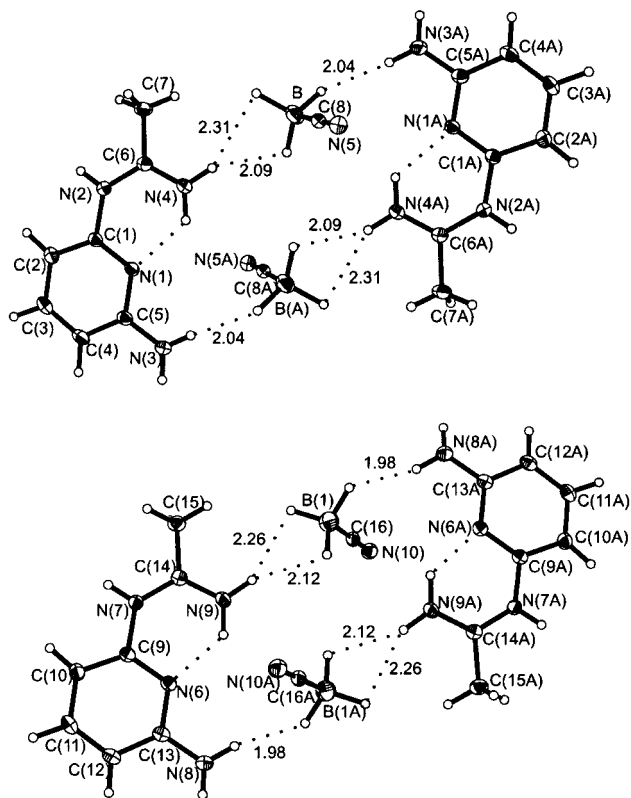
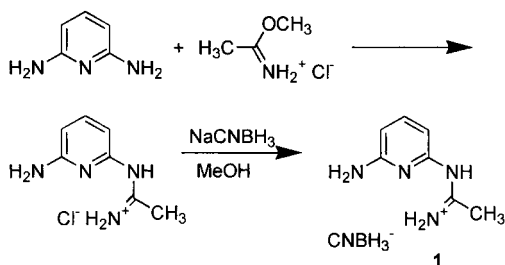


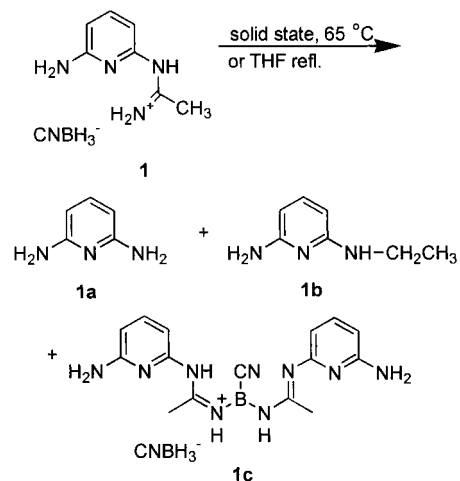
Figure 1. Crystal structure of NAPA H₃BCN showing the close H–H contacts in Å.

Scheme 3



2.04, 2.09, 2.31 Å, respectively. Applying the corrections for the N–H and B–H bonds that appear too short from X-ray compared to typical literature values, these H–H contacts become 0.1–0.15 Å shorter. This is well below the 2.4 Å van der Waals contact radius, implying strong and specific interactions. The NH \cdots H–B angles are strongly bent, ranging between 91.6° and 126.3° with an average of 108.2°, while the N–H \cdots HB angles are larger (range 148.1–175.6°; average 158.5°), which is characteristic for dihydrogen bonds.³ Conventional CN \cdots H–N (amidinium) H-bonds provide links between dimers of the same type. It thus appears that despite the less negative charge on the hydridic hydrogens (–0.18 vs –0.27 by Mulliken population analysis for MP2/6-311++G** wave functions), the CNBH₃[–] ion is capable of strong dihydrogen bonding, comparable to that of the BH₄[–] ion in this case, owing to the increased acidity of the proton donor partner. More important, the structure of this very first attempt showed two independent occurrences of the intended closed loop packing, with its potential for topochemical control. Decomposition in both solid and solution unfortunately led to complex mixtures (Scheme 4) via the unwanted reduction of the amidine group by the cyanoborohydride, which accounts for the majority of the decomposition products¹¹ identified by MS, ¹H, ¹³C, and

Scheme 4



¹¹B NMR. Although the decomposition product ratios were slightly different in the solid state and solution, we could not attribute that result to topochemical control, since the solid-state reaction occurred with partial liquefaction due to the low melting point of some of the products, relative to the temperature required for decomposition (~65 °C). Despite the lack of observable topochemical control, this system demonstrated the ability of CNBH₃[–] to form dihydrogen bonds and showed that the closed loop coordination is a viable packing arrangement that can be readily designed into dihydrogen-bonded systems.

Topochemical Control by Dihydrogen Bonding. Structure and Reactivity of NaBH₄·TEA (2). The complex of NaBH₄ with triethanolamine (TEA) was synthesized as a candidate for the globular cation strategy. The complex precipitated from a stirred mixture of NaBH₄ and TEA in THF as a white crystalline compound, which melts at 107–108 °C with decomposition and gas evolution. The X-ray powder diffraction pattern of the complex is unique and confirms the absence of NaBH₄. The ¹¹B and ²³Na solid-state MAS NMR chemical shifts are –47.9 and –9.9 ppm, respectively, 2.5 and 6.1 ppm downfield relative to sodium borohydride, indicating different environments for the BH₄[–] and Na⁺ ions. However, the B–H stretching vibration frequency for **2** (2288 cm^{–1}) is almost identical with the corresponding value in NaBH₄ (2291 cm^{–1}). The X-ray structure is shown in Figure 2. Each Na⁺ is hexacoordinated by the N and two O atoms from a TEA molecule and by three O atoms from the two neighboring TEA molecules, forming TEA·Na⁺ linear chains (Figure 2a). Two O atoms from each TEA molecule are shared by two adjacent Na⁺ cations, but the third oxygen only coordinates the next Na⁺ in the chain. Thus **2** is unlike the previously reported structures of TEA complexes where each cation was complexed by all four heteroatoms from TEA.¹² Multiple dihydrogen bonds connect the chains via the BH₄[–] anions, giving rise to extended two-dimensional layers (Figure 2b). Each BH₄[–] H-bonds with two OH groups in one chain and one OH group from the next chain in a total of five dihydrogen bonds. The H–H contacts from the three different OH sites are 1.94, 1.93, and 2.12 Å, and 2.16 and 2.13 Å in distance, respectively, the latter two being bifurcated H-bonds. Again, typical corrections for O–H and B–H bond lengths lead to H–H distances which are 0.15–0.2 Å shorter. The OH \cdots H–B

(11) Only one of the possible structures for **1c** is shown. However, at least three structures with the same molecular weight as indicated by MS, but different NMR spectra, were present in the final mixture.

(12) Naiini, A. A.; Pinkas, J.; Plass, W.; Young, V. G.; Verkade, J. G. *Inorg. Chem.* **1994**, *33*, 2137.

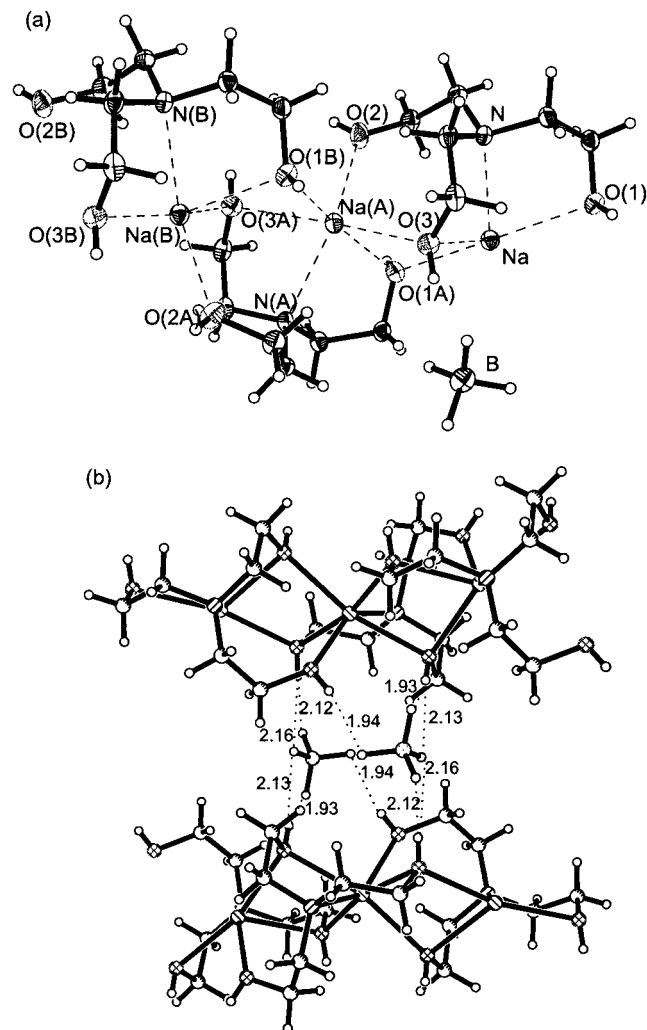


Figure 2. NaBH₄·TEA complex: (a) coordination of Na⁺; (b) dihydrogen bonds connecting the chains, with H-H contact distances in Å.

angles vary between 91.8 and 111.7° (average 98.0°) while the O-H...HB angles range between 143.9 and 166.7° (average 157.0°). There is no conventional H-bonding; instead all the hydroxylic protons point to the interchain space to form dihydrogen bonds with the borohydrides. This demonstrates once again that the dihydrogen bonding is important in defining the packing of the molecules in crystals.

Solid-state decomposition of NaBH₄·TEA at 82 °C¹³ under Ar or open atmosphere for 30–58 days resulted in a loss of 3 mol of H₂ for each mole of **2**, as indicated by the H⁻ content of the initial complex and final decomposed material. The rate of decomposition seems to be affected by different factors such as sample size, humidity, or the nature or pressure of the gas atmosphere above the solid,¹⁴ which is characteristic for many solid-state reactions.¹⁵ The resulting white solid is insoluble in common organic solvents and it does not melt up to 300 °C, suggesting a polymeric structure. Its ¹¹B solid-state MAS NMR shows a single peak at $\delta = -7.1$ ppm. X-ray powder diffraction

(13) Attempts to use higher temperatures for decomposition induced melting.

(14) Decomposition is slower under vacuum than under Ar and it is considerably faster in open atmosphere, probably due to the presence of humidity. The influence of different factors upon the decomposition rate of this and other dihydrogen-bonded systems is currently under study.

(15) (a) Gavezzotti, A.; Simonetta, M. *Chem. Rev.* **1982**, *82*, 1. (b) Sekiguchi, K.; Shirohata, K.; Sakata, O.; Suzuki, E. *Chem. Pharm. Bull.* **1984**, *32*, 1558.

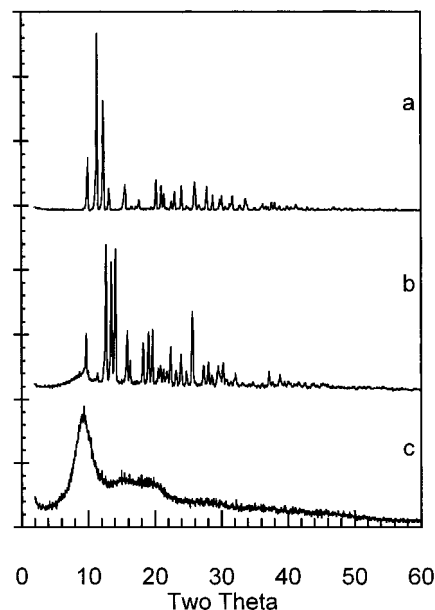


Figure 3. Progress of NaBH₄·TEA decomposition monitored by X-ray powder diffraction: (a) initial complex, (b) high-temperature polymorph, (c) final decomposed material.

of the same material exhibits only a semiamorphous phase with a broad peak at $2\theta = 9.4$ but no peaks corresponding to NaBH₄ or to the initial complex (Figure 3c). Furthermore, the ¹¹B NMR taken after hydrolysis of this material in neutral D₂O showed only traces of BH₄⁻, indicating the virtual absence of this boron species in the solid-state decomposition product. These data, correlated with the hydride content of the decomposed material (one H⁻ left), suggest a trialkoxyborohydride structure for the decomposed material. The B-H stretching frequency is shifted 5 cm⁻¹ relative to the initial complex (from 2288 to 2293 cm⁻¹). This is not a dramatic change, but it is not surprising since the variation of ν_{BH} in the BH_x(OR)_{4-x}⁻ series is generally small.¹⁶ The loss of 3 mol of H₂ is in agreement with the crystal structure of **2**, where each BH₄⁻ is H-bonded to three -OH groups, two from one chain and one from the next chain. This fact suggests a topochemical relationship between the starting and final materials. Additionally, the two -OH from the same chain in **2** belong to different adjacent TEA molecules. A topochemical reaction should therefore lead to a two-dimensional, extended covalent structure, and indeed, the peak at $2\theta = 9.4$ in the powder XRD (Figure 3c) corresponds to a *d* spacing of 9.41 Å in a layered structure. This value is very close to the 9.24 Å interlayer distance in the initial NaBH₄·TEA. Monitoring the solid-state decomposition by X-ray powder diffraction (Figure 3) and H⁻ analysis revealed a slow (~ 2 weeks), reversible phase transition of the initial complex, prior to any H₂ loss. The IR spectrum for this high-temperature polymorph shows the B-H stretching vibration at 2291 cm⁻¹ and the ¹¹B solid-state MAS NMR spectrum shows a chemical shift at -51.4 ppm. Structure elucidation of this high temperature crystalline intermediate, which somewhat complicates the topochemical relationship between the initial and final structures, would provide useful insight into the intimate mechanism of conversion from the dihydrogen bonding to the covalent networks. Unfortunately, only the low-temperature polymorph of **2** has been obtained in recrystallization attempts to date.

(16) (a) Ashby, E. C.; Dobbs, F. R.; Hopkins, H. P. *J. Am. Chem. Soc.* **1975**, *97*, 3158. (b) Kadlec, V.; Hanzlik, J. *Collect. Czech. Chem. Commun.* **1974**, *39*, 3200.

An indication for topochemical control is that different reaction products or stereoselectivity are observed in the solid state and solution or melt. Therefore, we also studied decomposition of **2** in DMSO solution and in the melt. A solution of **2** in DMSO was stirred and heated under Ar at 110 °C¹⁷ for 55 h. Like the solid-state decomposition product, the resulting precipitate is insoluble in common organic solvents and does not show any melting below 300 °C. However, H⁻ analysis and IR showed that this compound has virtually no hydridic hydrogen left.¹⁸ Its ¹¹B solid-state MAS NMR chemical shift is slightly different from the solid-state decomposition material ($\delta = -5.0$ ppm). No other product of decomposition was found by ¹¹B NMR of the mixture resulting from a parallel reaction run in DMSO-*d*₆, BH₄⁻ being the only boron species left in solution. On the other hand, when the solid-state decomposition product was stirred in DMSO under the same conditions, no change was observed in the hydridic content or IR spectrum, implying again different products for the solid and solution decompositions. This experiment demonstrated that unlike in the solid state, where the reaction stops at trialkoxyborohydride, decomposition of **2** in solution results in complete alcoholysis of BH₄⁻ to B(OR)₄⁻ as expected for a reaction in which the BH_x(OR)_{4-x}⁻ intermediates, which are more reactive than the starting borohydride, are mobile and therefore susceptible to disproportionation.¹⁹ Similarly, the reaction in the melt at 130 °C under Ar for 2 h resulted in complete alcoholysis of half²⁰ of the BH₄⁻ from the initial complex, NaBH₄ being the byproduct of decomposition as indicated by X-ray powder diffraction and ¹¹B NMR. It is remarkable that despite the considerably higher temperature of decomposition in the melt, only 2 mol of H₂ were lost compared to 3 in the solid state. The decomposition process in the solid state thus differs significantly from those in solution or melt. We believe that it is the particular packing of the molecules in the original crystal, dominated by H–H interactions, that induced the reaction to take place under topochemical control, leading to an otherwise inaccessible poly-trialkoxoborohydride structure.

Structure and Reactivity of NaCNBH₃·TEA (3). NaCNBH₃·TEA complex was synthesized to explore the influence of varying the hydridic donor partner upon the structure and solid-state reactivity of the dihydrogen-bonded systems. Due to the smaller negative charge on the hydridic hydrogens, the dihydrogen bonds were expected to make smaller contributions in defining the solid-state structure and reactivity, compared to the borohydride analogue. The complex was crystallized by slow evaporation of a 1:1 triethanolamine–NaCNBH₃ mixture in 2-propanol. The X-ray structure is shown in Figure 4. The Na⁺ cations are heptacoordinated by the four heteroatoms from one TEA molecule, the nitrogen from the cyanoborohydride and two oxygens from neighboring TEAs which bridge adjacent Na⁺ cations to form extended chains (Figure 4a), cross-linked by dihydrogen bonds. One H from each CNBH₃⁻ hydrogen bonds to a hydroxylic proton from another chain (Figure 4b) with an uncorrected H–H contact distance of 2.16 Å (OH···H–B angle = 100.6°; O–H···HB angle = 159.6°), forming a three-

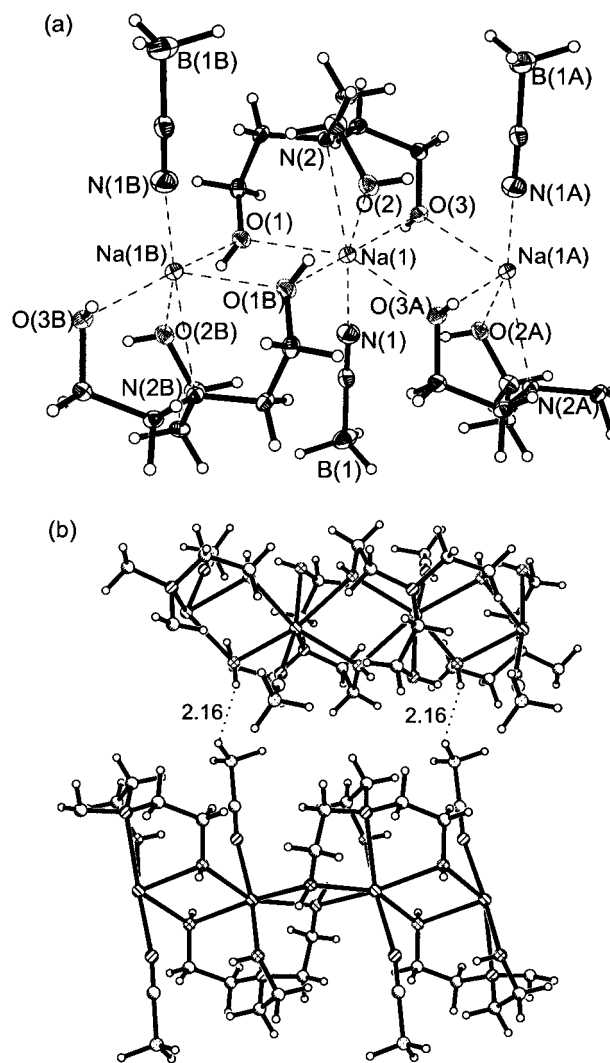


Figure 4. NaCNBH₃·TEA complex: (a) coordination of Na⁺; (b) dihydrogen bonds connecting the chains, with H–H contact distances in Å.

dimensional network. There are also O(1)–H···O(2) intrachain conventional H-bonds connecting neighboring TEA molecules. It appears that dihydrogen bonds are less important in the NaCNBH₃·TEA crystal packing than in the borohydride analogue, with its shorter H–H contacts and complete absence of conventional H-bonding. This difference is also reflected in the significantly different solid-state reactivity of the two complexes. While the borohydride complex melted at 107–108 °C with decomposition, the cyanoborohydride analogue melts at 85–86 °C, and it takes approximately 100 more degrees to finally start decomposing. Thus, close H–H contacts do not automatically confer solid-state reactivity; the relative acidity and basicity of the protonic and hydridic partners are also critical.²¹

Conclusions

1. Dihydrogen bonds can play an important role in defining solid-state structures, comparable to conventional hydrogen bonds. This was demonstrated by the crystal structures of all three compounds studied, where this new type of interaction

(17) The reaction was also carried out at 82 °C, the temperature used for the solid-state decomposition. The same product as at 110 °C was obtained, but the reaction was significantly slower.

(18) Attempts to measure the overall H₂ loss were not made because the rate of decomposition is very slow and the reaction could not be completed in a reasonable amount of time.

(19) Davis, R. E.; Gottbrath, J. A. *J. Am. Chem. Soc.* **1962**, *84*, 895.

(20) Two moles of H₂ were lost and ¹¹B NMR shows a ratio of BH₄/B(OR)₄ of approximately 1. Further heating at 130 °C for 5 days did not cause any additional H₂ loss. Even less H₂ was lost (~1/4) when a 1:1 mixture of NaBH₄ and TEA was allowed to react at 130 °C.

(21) Precise estimates of the basicities of BH₄⁻ and BH₃CN⁻ are unavailable, but the bimolecular rate constants for their H₃O⁺-catalyzed hydrolysis are ~10⁶ and 10⁻² L/(mol s), respectively, which may be translated into a p*K*_a difference of ~8 units. See: Davis, R. E.; Bromels, E.; Kibby, C. L. *J. Am. Chem. Soc.* **1962**, *84*, 885. Kreevoy, M. M.; Hutchins, J. E. C. *J. Am. Chem. Soc.* **1969**, *91*, 4329.

significantly influenced the arrangement of molecules in crystals. With its capacity to control crystal packing, dihydrogen bonding, like traditional H-bonding, finds its place among the tools that chemists can use for crystal engineering, as illustrated by the successful assembly of the desired closed loop dimers in NAPA H₃BCN. The additional feature that makes this new sort of H-bonding particularly interesting is the ability to react, trading the weak H...H interactions for strong covalent bonds. As a direct consequence of this character, dihydrogen bonding has the potential to induce topochemical control, providing access to new materials otherwise not achievable.

2. The NaBH₄·TEA complex has demonstrated the topochemical control concept. Its crystal structure shows multiple dihydrogen bonds between BH₄⁻ and the three OH groups from TEA. Loss of 3 mol of H₂ leads to a polymeric trialkoxyborohydride structure, whereas solution or melt decompositions yield NaBH₄ and a polymeric borate with no hydridic hydrogen left. Interestingly, more H₂ is lost in the solid-state decomposition than in the melt, despite the much higher reaction temperature in the latter (130 °C vs 82 °C). However, the product of the solid-state decomposition showed poor crystallinity and the reaction times were exasperatingly long due to the relatively low temperature required for decomposition to avoid melting.

3. In addition to close H—H contacts, the relative acidity/basicity of the proton—hydride pairs significantly affect the solid-state reactivity of the dihydrogen-bonded systems. This was demonstrated by changing the H⁻ donor from BH₄⁻ to CNBH₃⁻ in the TEA complexes, which resulted in substantial decreases in dihydrogen bonding and solid-state reactivity. More acidic cations should enhance the solid-state reactivity of these systems, resulting in faster decompositions at lower temperatures, and thus lower molecular mobility in the crystal, so that the initial three-dimensional regularity dictated by the H—H interactions may carry over to the final covalent product.

In summary, careful design of dihydrogen-bonded systems, with appropriate consideration of geometry and matching of acidity and basicity of the protonic and hydridic partners, is capable of conferring topochemical control on the H₂ loss which replaces the weak interactions with strong covalent bonds. This strategy thus offers real prospects for equipping chemistry with tools for rational synthesis of new materials with crystalline three-dimensional covalent structures.

Experimental Section

Sodium cyanoborohydride (NaCNBH₃) and sodium borohydride (NaBH₄) were purchased from Aldrich and used without further purification. *N*-[2-(6-Aminopyridyl)]acetamide hydrochloride was prepared by a literature procedure.²² Tetrahydrofuran (THF) was distilled from Na/benzophenone under Ar. 2-Propanol was distilled from CaH₂ under Ar. Dimethyl sulfoxide (DMSO) was distilled from BaO under vacuum and stored over 4 Å molecular sieves. Melting points were taken on a Thomas-Hoover instrument and are uncorrected. FT-IR spectra were measured on a Perkin-Elmer Spectrum 2000 instrument. ¹H NMR spectra were recorded on a Gemini-300 instrument. ¹³C NMR and ¹¹B (96.23 MHz) NMR spectra were recorded on a Varian VXR-300 instrument. ¹¹B (128.33 MHz) and ²³Na (105.81 MHz) solid-state MAS NMR spectra were measured on a Varian VXR-400 instrument. ¹¹B solution NMR chemical shifts were referenced to B(OCH₃)₃ in CDCl₃. ¹¹B solid-state MAS NMR chemical shifts were referenced to solid boric acid and ²³Na chemical shifts were referenced to solid NaCl. A negative sign indicates chemical shifts upfield from references. X-ray powder diffraction measurements were conducted on a Rigaku-Denki RW400F2 diffractometer with monochromatic Cu Kα radiation, oper-

ated at 45 kV and 100 mA. Analysis of H⁻ content was done by measuring the volume of H₂ evolved on treatment with diluted HCl.

***N*-[2-(6-Aminopyridyl)]acetamide Hydrochloride (1).** *N*-[2-(6-Aminopyridyl)]acetamide hydrochloride (2.61 g, 0.014 mol) and 0.88 g (0.014 mol) of NaCNBH₃ were dissolved in 65 mL of methanol and the resulting clear solution was left standing at room temperature for 12 h. After the removal of methanol in vacuo, 20 mL of THF was added and the solution was filtered. The filtrate was concentrated in vacuo and 100 mL of CH₂Cl₂ was added. The resultant precipitate was collected to yield 2 g (75%) of product as a white solid. X-ray quality crystals were grown by diffusion of cyclohexane vapors into a 2-propanol solution of **1**. Mp 119–120 °C; IR (KBr) ν_{BH} = 2338, 2219 cm⁻¹, ν_{CN} = 2168 cm⁻¹; ¹H NMR (DMSO-*d*₆) δ 7.47 (t, *J* = 8 Hz, 1 H), 6.52 (s, 2 H), 6.26 (t, *J* = 8 Hz, 2H), 2.31 (s, 3 H), 0.21 (q, *J*_{BH} = 88.5 Hz, 3 H); ¹¹B NMR (DMSO-*d*₆) δ -55.95 (q, *J*_{BH} = 88.8 Hz); ¹³C NMR (DMSO-*d*₆) δ 164.0, 158.1, 150.6, 140.1, 104.4, 100.1, 20.0. Anal. Calcd for C₈H₁₄N₃B: C, 50.26; H, 7.33; N, 36.65. Found: C, 49.64; H, 7.57; N, 36.11.

NaBH₄·TEA (2). A mixture of 0.38 g (0.01 mol) of NaBH₄ and 2.8 mL (0.02 mol) of triethanolamine in 25 mL of THF was stirred at room temperature for 2 h. Filtration of the precipitate obtained and washing with THF yielded 0.95 g (51%) of **2**. Crystals suitable for X-ray crystallography were obtained by slow cooling of a solution of **2** in 2-butanol from room temperature to -25 °C. Mp 107–108 °C dec; IR (KBr) ν_{BH} = 2288 cm⁻¹; ¹H NMR (pyridine-*d*₆) δ 6.68 (br, 3H), 3.87 (t, *J* = 5.1 Hz, 6 H), 2.67 (t, *J* = 5.1 Hz, 6 H), 1.30 (q, *J*_{BH} = 81.3 Hz); ¹¹B NMR (DMSO-*d*₆) δ -49.28 (quintet, *J*_{BH} = 81.4 Hz); ¹¹B MAS NMR (6000 Hz) δ -47.9 (Δν_{1/2} = 1826 Hz); ¹³C NMR (DMSO-*d*₆) δ 58.9, 56.9; ²³Na MAS NMR (6029 Hz) δ -9.9 (Δν_{1/2} = 1649 Hz). Anal. Calcd for C₆H₁₉NO₃BNa: C, 38.50; H, 10.16; N, 7.49. Found: C, 38.09; H, 10.47; N, 7.39; H⁻ content, 4.11.

NaCNBH₃·TEA (3). A mixture of 0.63 g (0.01 mol) of NaCNBH₃ and 1.4 mL (0.01 mol) of triethanolamine in 30 mL of 2-propanol was stirred at room temperature for 2 h. The undissolved material was filtered out and the 2-propanol was slowly evaporated from the filtrate with a gentle stream of nitrogen. When almost dry, 50 mL of CH₂Cl₂ was added and the white solid was collected. Yield 1.1 g (52%). X-ray quality crystals were grown by slow evaporation of a solution of **3** in 2-propanol. Mp 85–86 °C; IR (KBr) ν_{BH} = 2341 cm⁻¹, ν_{CN} = 2180 cm⁻¹; ¹H NMR (CD₃CN-*d*₆) δ 3.55 (t, *J* = 5.4 Hz, 6 H), 3.46 (s, 3 H), 2.52 (t, *J* = 5.4 Hz, 6 H), 0.26 (q, *J*_{BH} = 88.6); ¹¹B NMR (DMSO-*d*₆) δ -55.9 (q, *J*_{BH} = 88.6); ¹³C NMR (DMSO-*d*₆) δ 59.0, 56.9. Anal. Calcd for C₇H₁₈N₂O₃BNa: C, 39.62; H, 8.49; N, 13.21. Found: C, 38.73; H, 9.23; N, 13.21.

Decomposition of NaBH₄·TEA in DMSO. A solution of 0.5 g of **2** in 10 mL of DMSO was heated at 110 °C under Ar for 55 h. The resulting precipitate was collected and washed with CH₂Cl₂ to yield 0.17 g of a white solid insoluble in common organic solvents. Mp > 300 °C; IR (KBr) no B—H stretching vibration; ¹¹B MAS NMR (6000 Hz) δ -5.0 (Δν_{1/2} = 1559 Hz); ²³Na MAS NMR (6011 Hz) δ -13.5 (Δν_{1/2} = 2665 Hz). Anal. H⁻ content, 0.22.

Decomposition of NaBH₄·TEA in Melt. A 0.5 g sample of **2** was placed in a 21 × 50 mm vial and heated under Ar at 130 °C in an oil bath for 2 h. In about 1 min the solid melted with effervescence. After approximately another 10 min the melt solidified. The powder XRD confirmed the presence of NaBH₄. ¹¹B MAS NMR (5998 Hz) δ -2.3 (Δν_{1/2} = 1394 Hz, 1 B), -50.4 (Δν_{1/2} = 1017, Hz 1.2 B). Anal. H⁻ content, 2.03.

Solid-State Decomposition of NaBH₄·TEA. A 0.5–0.7 g sample of **2** was heated at 82 °C under Ar or open atmosphere in a 7 × 27 mm glass tube immersed in refluxing acetonitrile for 30–58 days. The resulting white solid is insoluble in common organic solvents and it does not melt up to 300 °C. The powder XRD shows a single phase with a broad peak at 2θ = 9.4 but no NaBH₄ or **2**. IR (KBr) ν_{BH} = 2387, 2293, 2226 cm⁻¹; ¹¹B MAS NMR (6058 Hz) δ -7.1 (Δν_{1/2} = 1390 Hz); ²³Na MAS NMR (6004 Hz) δ -14.6 (Δν_{1/2} = 2769 Hz). Anal. N/B/Na = 1/1/0.96; H⁻ content, 1.05–1.38.

X-ray Structure Determination of 1, 2, and 3. X-ray crystallographic measurements were carried out on a Siemens SMART CCD diffractometer with graphite-monochromated Mo Kα radiation (λ = 0.71073 Å), operated at 50 kV and 40 mA. The structures were solved

(22) Bernstein, J.; Stearns, B.; Shaw, E.; Lott, W. A. *J. Am. Chem. Soc.* **1947**, *69*, 1151.

by direct methods and refined on F^2 with the SHELXTL software package.²³ Absorption corrections were applied for **2** by using SADABS, part of the SHELXTL software package. All non-hydrogen atoms were refined anisotropically. Hydrogen atoms were located from difference Fourier maps and refined isotropically for all three structures.

Acknowledgment. This work was supported by Grant No. N508 from the MSU Center for Fundamental Materials Research

(23) *SHELXTL: Structure Analysis Program 5.1*; Bruker AXS, Inc., Madison, WI, 1997.

(CFMR). We are grateful to Dr. Dimitris Papoutsakis and Dr. Donald L. Ward for X-ray assistance.

Supporting Information Available: Tables with full X-ray details, atomic coordinates, isotropic and anisotropic displacement parameters, bond lengths, and angles for **1–3** (20 pages, print/PDF). See any current masthead page for ordering information and Web access instructions.

JA982959G